Effects of Core Mutations on the Folding of a β-Sheet Protein: Implications for Backbone Organization in the I-State[†]

Mark Lorch,* Jody M. Mason, Anthony R. Clarke, and Martin J. Parker[‡]

Department of Biochemistry, School of Medical Sciences, University of Bristol, University Walk, Bristol BS8 1TD, U.K.

Received July 23, 1998; Revised Manuscript Received October 21, 1998

ABSTRACT: A series of core mutations were introduced into β-strand segments of an immunoglobulin fold (the isolated first domain of CD2, CD2.d1) to examine their influence on the rapidly formed intermediate state (I-state) which transiently accumulates in the folding reaction [Parker, M. J., and Clarke, A. R. (1997) *Biochemistry 36*, 5786−5794]. The residue changes were chemically conservative, each representing the removal of one or two methylene groups from aliphatic side chains. Predictably, the mutations destabilize the folded state with respect to the unfolded state by about 1.1 ± 0.7 kcal mol^{-1} per methylene group removed. However, when the folding reaction is dissected by transient kinetic analysis into its component steps, six out of the nine mutations lead to a stabilization of the I-state. The direction and magnitude of these effects on the global stability of the transient intermediate are well correlated with changes in secondary structure propensity occasioned by the substitutions. The results show that, although side chain interactions are extremely weak in this early phase of folding, the β-strand conformation of the polypeptide chain is established. In the next phase of the reaction, the rate-limiting transition state is attained by the formation of a tightly localized hydrophobic nucleus which includes residues V30, I18, and V78. Interestingly, in almost all immunoglobulin domains of extracellular proteins, the latter pair are cysteine residues which form a disulfide bridge.

While it has long been maintained that the chief driving force in achieving and maintaining the native state of protein molecules is the hydrophobic interaction (*1*, *2*), the role played by other interactions, such as main chain torsion angle preferences and backbone hydrogen bonding, remains a subject of some debate. The emphasis placed on the relevance of these interactions has a marked influence on how we view the process of protein folding. In hierarchic models of protein folding, for example, main chain torsion angle preferences and short-range backbone hydrogen bonding interactions play an important role in predisposing parts of the sequence to forming native-like elements of secondary structure in the earliest stages of folding (*3*−*5*). In contrast, hydrophobic collapse models view the early stages of folding as being driven by the global and random association of nonpolar groups (*6*, *7*). The greatly reduced number of possible chain configurations in these compact states is then proposed to reduce the scale of the search problem (*8*).

Despite the cooperative nature of the folding mechanism, there is an increasing number of examples of proteins where folding begins with the rapid formation of well-populated intermediates (*9*, *10*). Such intermediates are compact and contain extensive native-like secondary structure. They do, however, lack the intimate side chain contacts characteristic of the native state and are still partially hydrated. Given the complexity of the search problem, studying these transient species offers an opportunity to understand the basic sequence determinants for limiting conformational freedom. The mechanistic relevance of these species has been brought into question however. While some maintain that these species are an essential and relevant part of the folding process (*9*, *10*), others argue that they are misfolded structures which actually inhibit the folding reaction (*11*, *12*). Either view depends, to a large degree, on the extent to which the types of interaction listed above direct the chain toward its native topology in these early stages of structure acquisition. Resolution of these arguments therefore demands the detailed elucidation of the structural, energetic, and dynamic properties of these rapidly formed intermediates.

The 98-residue, N-terminal domain of rat CD2 (CD2.d1)[1] is an all-β protein belonging to the IgG superfamily but, unusually, contains no disulfide bridge (*13*). Kinetic studies reveal that this protein folds via the rapid formation of an intermediate which precedes the rate-limiting formation of the folded state (*14*). The structure of this state has been extensively probed by hydrogen−deuterium exchange studies (*15*, *16*), and its thermodynamic properties have been assessed by the temperature dependence of kinetic parameters (*17*). Taken together, the results of these experiments imply a high degree of native-like chain organization in the I-state. In a further effort to address the issues raised above, we now

[†] This work was supported by a project grant from the BBSRC (U.K.) and equipment funding from the Wellcome Trust. M.J.P. is a Wellcome Trust International Prize Traveling Fellow. A.R.C. is a Lister Institute Research Fellow.

* To whom correspondence should be addressed.

[‡] Current address: Department of Molecular and Cell Biology, Division of Biochemistry and Molecular Biology, 229 Stanley Hall, University of California, Berkeley, CA 94720.

[1] Abbreviations: CD2.d1, 98-residue, N-terminal domain of the cell surface receptor protein CD2 from rats; GST, glutathione *S*-transferase; GuHCl, guanidine hydrochloride; TEA, triethanolamine hydrochloride; WT, wild type CD2.d1.

10.1021/bi9817820 CCC: $18.00
Published on Web 01/05/1999

examine the effect of side chain truncations on the stability of both the I-state and the rate-limiting transition state in the folding reaction.

EXPERIMENTAL PROCEDURES

Source of Protein. All mutants of CD2.d1 were generated using the one-sided overlap extension method (*18*) using a Perkin-Elmer DNA thermal cycler and cloned into the pGEX-2T glutathione *S*-transferase (GST) fusion vector (Pharmacia). Resulting constructs were transformed into competent *Escherichia coli* HB2151 cells (Pharmacia). Plasmid DNA from transformants overexpressing GST fusion proteins, as assessed by SDS−PAGE, was prepared and sequenced to check for incorporation of correct mutant codons and to ensure no random errors had been incorporated into the rest of the gene. Oligonucleotides used for mutagenesis and sequencing were obtained from Cruachem Ltd. Sequencing of DNA was performed by the chain termination procedure, using a Du Pont Genesis 2000 automated sequencer.

Wild type and mutant proteins were prepared and purified as described previously (*14*). Protein concentrations were estimated by UV absorption of aromatic residues at 280 nm [$\epsilon = 5500\ M^{-1}\ cm^{-1}$ for tryptophan (two residues) and 1100 $M^{-1}\ cm^{-1}$ for tyrosine (two residues)].

Equilibrium and Kinetic Folding and Unfolding Measurements. Guanidine hydrochloride (GuHCl) (Sigma Chemical Co.)-induced equilibrium unfolding profiles were measured by fluorescence spectroscopy, as described previously (*14*). The GuHCl-dependent folding and unfolding rates were measured by fluorescence stopped-flow spectroscopy, as described previously (*14*). Both equilibrium and kinetic measurements were carried out in 50 mM triethanolamine hydrochloride (TEA) (Boehringer Mannheim) (pH 7.5). Sodium sulfate (Na_2SO_4) (Sigma Chemical Co.) was added to GuHCl and protein solutions at appropriate concentrations to give the denaturant activities defined below.

All reaction solutions were maintained at 25 °C using thermostated circulating water baths and were monitored continuously with a sensitive thermocouple. From this, the fluctuation in temperature was determined to be no more than ±0.1 °C.

ANALYTICAL PROCEDURES

Denaturant Activity. For the analysis of equilibrium and kinetic data, the guanidine hydrochloride concentration ([GuHCl]), in the presence and absence of Na_2SO_4, is converted to a common molar denaturant activity (D) by the following relationship:

$$D = [C_{0.5}[\mathrm{GuHCl}]/(C_{0.5} + [\mathrm{GuHCl}])] - 2.6[Na_2SO_4] \quad (1)$$

where $C_{0.5}$ is a denaturation constant with a value of 7.5 M (*19*).

This treatment has been dealt with in detail elsewhere (*14*, *15*, *19*), and the coefficient of 2.6 is derived from the linear relationship between Na_2SO_4 concentration and denaturant activity between 0 and 0.4 M (i.e., solutions of 0, 0.1, 0.2, 0.3, and 0.4 M Na_2SO_4 give molar denaturant activities of 0, −0.27, −0.51, −0.78, and −1.03 M, respectively).

Treatment of Equilibrium Data. Equilibrium fluorescence profiles were fitted to the equation

$$I = \alpha_F I_F + \alpha_U I_U \quad (2)$$

with temporary variables

$$K_{F/U} = K_{F/U(W)} \exp(m_U D)$$

$$\alpha_F = K_{F/U}/(1 + K_{F/U})$$

$$\alpha_U = 1 - \alpha_F$$

where α_F and α_U are the fractional populations of molecules in the folded (F) and unfolded (U) states, respectively, I, I_F, and I_U are the fluorescence intensities (measured, folded, and unfolded, respectively), $K_{F/U}$ is the equilibrium constant ([F]/[U]) at a given denaturant activity, $K_{F/U(W)}$ is this equilibrium constant in water, and m_U is the exponential reduction in $K_{F/U}$ as a function of denaturant activity (it has units of M^{-1}).

Treatment of Kinetic Data. The transients of fluorescence intensity (I) versus time, which are single, first-order processes, in both the folding and unfolding directions, were fitted to the equation $I = I_a[1 - \exp(-kt)] + I_o$ for rising intensities (where I_a is the fluorescence amplitude of the reaction, k is the observed rate constant for relaxation, and I_o is the initial intensity) and to $I = I_a \exp(-kt) + I_f$ for decreasing intensities (where I_f is the final fluorescence intensity).

Rate profiles [observed rate constant (k_{obs}) vs denaturant activity] were fitted to the equation

$$k_{obs} = k_{F-I} + k_{I-F}/(1 + 1/K_{I/U}) \quad (3)$$

where k_{I-F} and k_{F-I} are rate constants describing the forward and reverse transitions, respectively, between the folded and intermediate (I) states and $K_{I/U}$ is the equilibrium constant ([I]/[U]) for the rapid interconversion of the intermediate and unfolded states (*19*). In the fitting routine, the following temporary variables were used:

$$k_{F-I} = k_{F-I(W)} \exp(-m_t D)$$

$$k_{I-F} = k_{I-F(W)} \exp[(m_I - m_t)D]$$

$$K_{I/U} = K_{I/U(W)} \exp[(m_U - m_I)D]$$

where the subscript W describes the rate and equilibrium constants in water, t is the I-to-F transition state, and the m parameters describe the shifts in the stabilities of each state (designated by the subscript) as a function of the denaturant activity (units of M^{-1}). These are measured relative to the values of the folded state, and hence, the values are negative.

All data were fitted using the Grafit analysis software (Erithracus Software). When kinetic data were fitted to eq 3, proportional weighting was used so that the fitted values took account of rate constants equally across the whole range.

Calculation of β-Propensity. A set of 123 globular and four membrane protein chains, with less than 25% pairwise similarity and whose crystal structures are solved to a resolution of ≤2.5 Å (*20*), was extracted from the Brookhaven Protein Data Bank. From this data base, 254 terminal residues, 69 poorly defined residues, and a seleninic acid residue were removed. ϕ and ψ angles were assigned to the remaining 23 640 residues in this data base using the

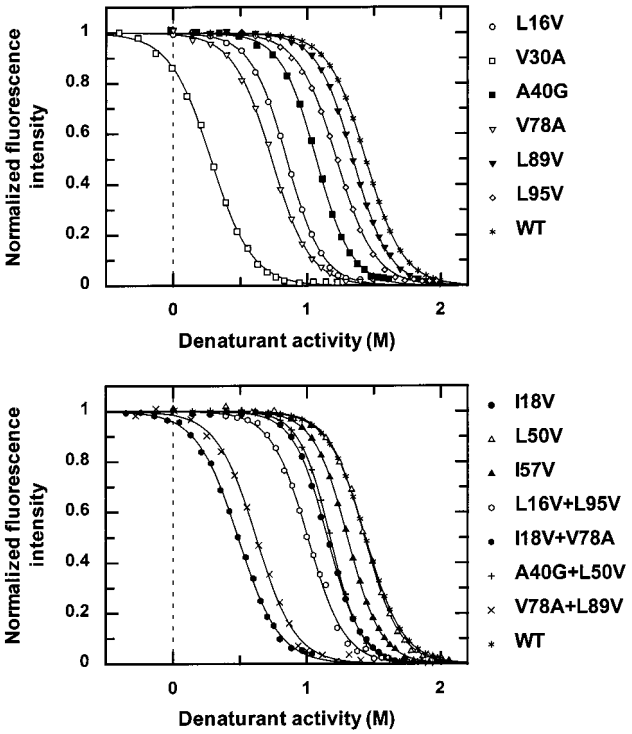

FIGURE 1: Equilibrium unfolding. The GuHCl-induced equilibrium unfolding profiles (25 °C and pH 7.5) for the CD2.d1 mutant proteins are shown in two plots for clarity. The fluorescence intensities have been normalized for comparative purposes and are plotted against denaturant activity, calculated using eq 1 (see Analytical Procedures and Results). The data have been fitted to eq 2, which describes a two-state equilibrium folding−unfolding mechanism (fits shown as continuous curves). No baseline corrections have been applied to the data. The calculated values of $K_{F/U(W)}$ and m_U are given in Table 1. The wild type (WT) data are reproduced from ref *16*. These unfolding profiles are highly reproducible. In fact, repeated experiments in which both freshly prepared protein and solutions were used provide identical folding parameters, within the fitting uncertainties (see Table 1).

Procheck program. The β-region of the ϕ and ψ distribution was defined, by inspection, as follows: $-180 < \phi < -28$, $53 < \psi < 180$, and $-180 < \psi < -155$.

For a given residue, the quasi-equilibrium constant for ϕ and ψ angles in the β-region (K_β) is defined as

$$K_\beta = N_\beta/(N_{total} - N_\beta) \quad (4)$$

where N_β is the number of ϕ and ψ angles in the β-region and N_{total} is the total number of occurrences in the database. For the residues studied here, glycine, alanine, valine, leucine, and isoleucine, the values of K_β are 0.24, 0.53, 1.48, 0.71, and 1.25, respectively.

RESULTS

Folding Pathway of CD2.d1. The folding−unfolding reaction of CD2.d1 is conveniently monitored by changes in the fluorescence emission properties of its two tryptophan residues, at positions 7 and 32 in the sequence. The GuHCl-induced equilibrium unfolding profile of CD2.d1 reveals that the only species significantly populated at equilibrium are the fully folded (F) and fully unfolded (U) states (*14*; see Figure 1). The dependence of the observed relaxation rate for folding or unfolding (k_{obs}), measured by stopped-flow fluorescence (see Figure 2), reveals the presence of a

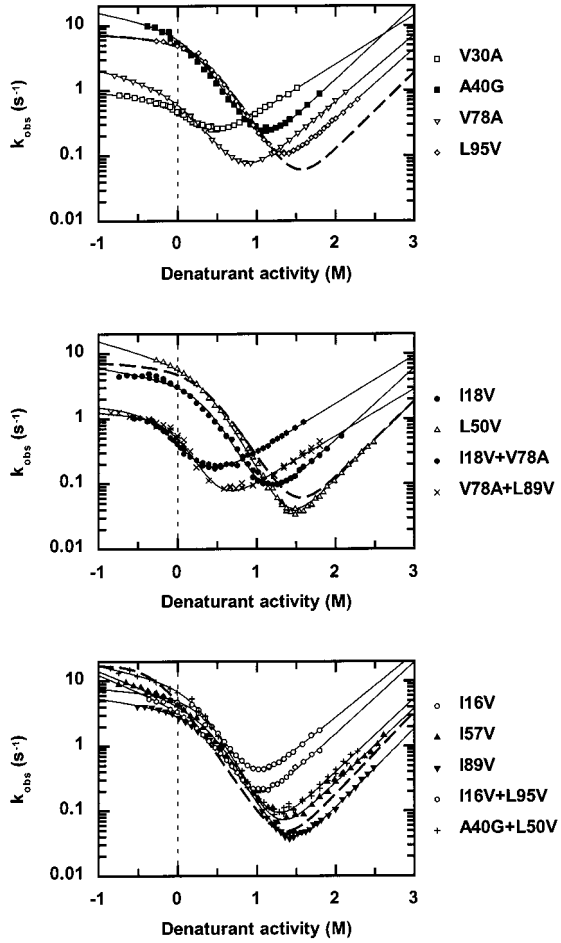

FIGURE 2: Folding dynamics. Rate profiles [observed relaxation rate (k_{obs}) vs denaturant activity] collected for the mutant CD2.d1 proteins (25 °C and pH 7.5) are shown here in three plots for clarity. The data have been fitted to eq 3 (fits shown as continuous curves). The calculated values of $k_{I-F(W)}$, $k_{F-I(W)}$, $K_{I/U(W)}$, m_U, m_I, and m_t are given in Table 1. The wild type (WT) curve (thick dashed curve) has been reproduced from ref *16*. As with the equilibrium data, these rate profiles are highly reproducible; experiments that were repeated in which both freshly prepared protein and solutions were used provide identical folding parameters, within the measured fitting uncertainties (see Table 1).

transiently populated intermediate (I), however, which is formed in the dead time of a conventional stopped-flow experiment (~1 ms); i.e., the rate of formation of I from U is greater than 10^3 s^{-1} (*14*, *15*).

The folding reaction of CD2.d1 is most simply described therefore by Scheme 1:

Scheme 1

$$U \overset{K_{I/U}}{\rightleftharpoons} I \underset{k_{F-I}}{\overset{k_{I-F}}{\rightleftharpoons}} F$$

where $K_{I/U}$ is the equilibrium constant ([I]/[U]) for the rapid U-to-I transition and k_{I-F} and k_{F-I} are the folding and unfolding rates, respectively, associated with the rate-limiting I-to-F transition. Values for these equilibrium and rate constants in water [$K_{I/U(W)}$, $k_{I-F(W)}$, and $k_{F-I(W)}$] are obtained by fitting the rate data in Figure 2 to eq 3. Three other physically relevant parameters obtained from these data are m_U, m_I, and m_t, which measure how the free energies of U, I, and t (I-to-F transition state), relative to that of the F-state, vary with denaturant concentration. These *m* values provide

Table 1: Equilibrium and Kinetic Folding Parameters

mutant	$K_{F/U(W)}$[a]	$K_{I/U(W)}$	$k_{I-F(W)}$ (s^{-1})	$k_{F-I(W)}$ (s^{-1})	m_U[b] (M^{-1})	m_I (M^{-1})	m_t (M^{-1})	ϕ and ψ[c] (deg)
WT[d]	$(4.31 \pm 1.20) \times 10^4$	3.55 ± 0.61	6.02 ± 0.31	$(5.38 \pm 1.00) \times 10^{-4}$	-7.08 ± 0.10	-2.91 ± 0.17	-2.72 ± 0.06	–
L16V	$(1.03 \pm 0.48) \times 10^3$	4.80 ± 2.00	5.80 ± 0.60	$(2.70 \pm 0.50) \times 10^{-2}$	-7.40 ± 0.40	-2.70 ± 0.30	-2.30 ± 0.12	−98.13 and 106.55
I18V	$(5.95 \pm 1.50) \times 10^3$	4.80 ± 0.60	3.60 ± 0.16	$(2.90 \pm 0.60) \times 10^{-3}$	-7.81 ± 0.20	-3.10 ± 0.13	-2.60 ± 0.13	−74.67 and 119.83
V30A	11.0 ± 3.0	1.26 ± 0.30	0.69 ± 0.07	$(7.70 \pm 0.40) \times 10^{-2}$	-6.50 ± 0.30	-2.00 ± 0.10	-1.70 ± 0.04	−146.16 and 129.11
A40G	$(2.34 \pm 0.45) \times 10^3$	2.14 ± 0.33	8.70 ± 0.50	$(8.02 \pm 0.80) \times 10^{-3}$	-7.41 ± 0.10	-3.20 ± 0.15	-2.60 ± 0.06	−158.74 and 150.04
L50V	$(8.05 \pm 2.11) \times 10^4$	4.80 ± 0.30	6.80 ± 0.32	$(4.00 \pm 1.02) \times 10^{-4}$	-8.00 ± 0.20	-3.60 ± 0.18	-2.80 ± 0.06	−125.28 and 133.27
I57V	$(2.07 \pm 0.51) \times 10^4$	6.30 ± 0.70	4.60 ± 0.21	$(1.40 \pm 0.30) \times 10^{-3}$	-7.90 ± 0.08	-3.80 ± 0.12	-2.60 ± 0.08	−109.42 and 125.87
V78A	$(2.60 \pm 0.25) \times 10^2$	1.77 ± 0.08	0.90 ± 0.02	$(6.20 \pm 0.31) \times 10^{-3}$	-6.90 ± 0.18	-3.20 ± 0.05	-2.30 ± 0.03	−114.18 and 138.33
L89V	$(3.40 \pm 0.90) \times 10^4$	3.91 ± 0.40	3.50 ± 0.10	$(4.02 \pm 1.00) \times 10^{-4}$	-7.40 ± 0.05	-3.20 ± 0.10	-2.80 ± 0.07	−157.61 and 149.66
L95V	$(1.20 \pm 0.24) \times 10^4$	5.10 ± 0.90	5.90 ± 0.30	$(2.50 \pm 0.20) \times 10^{-3}$	-7.50 ± 0.09	-2.70 ± 0.20	-2.50 ± 0.05	−92.68 and 116.76
L16V/L95V	$(1.42 \pm 0.25) \times 10^3$	5.11 ± 0.20	4.50 ± 0.17	$(8.40 \pm 1.00) \times 10^{-3}$	-7.30 ± 0.30	-3.40 ± 0.15	-2.60 ± 0.10	–
I18V/V78A	8.00 ± 0.50	0.37 ± 0.06	1.30 ± 0.10	$(6.00 \pm 0.30) \times 10^{-2}$	-6.40 ± 0.20	-1.90 ± 0.20	-1.70 ± 0.05	–
A40G/L50V	$(1.28 \pm 0.36) \times 10^4$	3.00 ± 0.70	9.00 ± 0.75	$(2.10 \pm 0.30) \times 10^{-3}$	-7.90 ± 0.10	-3.30 ± 0.10	-2.60 ± 0.08	–
V78A/L89V	44.0 ± 21.0	0.84 ± 0.34	1.00 ± 0.23	$(2.01 \pm 0.20) \times 10^{-2}$	-7.30 ± 0.50	-1.80 ± 0.30	-1.70 ± 0.80	–

[a] $K_{F/U(W)}$ values averaged from equilibrium and kinetic data [$K_{F/U(W)} = [k_{I-F(W)}/k_{F-I(W)}]K_{I/U(W)}$]. [b] m_U values averaged from equilibrium and kinetic data. [c] ϕ and ψ angles of the mutated residues calculated using the Procheck program. [d] Wild type (WT) data reproduced from ref *16*. Quoted errors are standard errors calculated from least-squares fits to the data (based on a 95% confidence limit). Accumulated standard errors were calculated using standard statistical formulas.

a qualitative measure of the relative degree to which hydrocarbon in each state is exposed to aqueous solvent (*19*, *21*−*23*); therefore, the magnitude of the *m* value will be roughly proportional to the amount of hydrocarbon buried in the core of the protein, and consequently should reflect its size. For example, CD2.d1 is 98 amino acids long and has an m_u value of -7.1 M^{-1}, compared to -21.9 M^{-1} for C-PGK (*24*), which is made up of 220 amino acids.

There is a nonlinear relationship between denaturant concentration and both the free energy of solvation of hydrocarbon (*22*, *25*, *26*) and the free energy of protein folding (*27*). To correct for this nonlinearity, the GuHCl concentration [GuHCl] is converted to denaturant activity (*D*) as described in detail elsewhere (*14*, *15*, *19*). The use of this linearized scale allows more reliable extrapolations to conditions where denaturant is absent, i.e., for the evaluation of rate and equilibrium constants in water.

Some of the mutations described in this study destabilize the I-state to such an extent that it is no longer populated in water alone [$K_{I/U(W)} < 1$]. To increase the population of the I-state, we employ the cosmotropic agent sodium sulfate (Na_2SO_4). This compound works in a manner analogous but opposite from that of GuHCl, increasing the free energy of solvation of hydrocarbon and consequently driving the folding reaction in favor of more compact, desolvated states. This compound has been used by others to determine the energetic properties of hydrophobic core mutants of ubiquitin (*28*) and for the evaluation of amide proton protection factors for the I-state of CD2.d1 (*15*, *16*). The molar ability of Na_2SO_4 to decrease the extent of hydrocarbon solvation has been scaled to the molar ability of GuHCl to increase it, allowing us to calculate the denaturant activity of Na_2SO_4 (see Analytical Procedures and ref *15*). This results in negative values of denaturant activity.

Folding Energetics of Mutants. We have constructed nine single and four double mutants in which buried aliphatic residues found in the β-strand segments of CD2.d1 have been replaced by smaller aliphatics. The ϕ and ψ angles of these residues in the folded state all lie within the β-region (see Table 1 and Analytical Procedures). The mutations were designed to cause minimal structural perturbation, involving the removal of only one or two methylene groups from the side chains of Ala, Val, Leu, and Ile residues. All of these mutations remove side chain−side chain interactions between nonpolar residues buried in the hydrophobic core of the folded state, as judged by inspection of the native crystal structure (*29*). The mutations were created with the view of carrying out Φ value analysis (*30*) and double-mutant cycle analysis (*31*) to measure the temporal development of side chain interactions during the folding reaction of CD2.d1.

The equilibrium unfolding profiles collected for these mutants are shown in Figure 1. All of the mutants exhibit an apparent two-state folding transition at equilibrium. The data therefore have been fitted to eq 2, and the calculated values of $K_{F/U(W)}$ and m_U are given in Table 1. With the exception of L50V, all the single mutations reduce the stability of the folded state, with values for the difference free energy change between F and U, $\Delta\Delta G_{F-U}$, ranging from -4.9 to -0.14 kcal mol^{-1} (see Table 2). These destabilizing effects are consistent with the loss of van der Waals interactions in the folded state and with the reduction of the exposed nonpolar surface area in the unfolded state. The

Table 2: Free Energy Changes[a]

mutant	$\Delta\Delta G_{F-U}$ (kcal mol^{-1})	$\Delta\Delta G_{I-U}$ (kcal mol^{-1})	$\Delta\Delta G_{t-U}$[b] (kcal mol^{-1})	Φ_I[c]	Φ_t[c]	$\Delta G_{int(F)}$[d] (kcal mol^{-1})	$\Delta G_{int(I)}$[d] (kcal mol^{-1})	$\Delta G_{int(t)}$[d] (kcal mol^{-1})
L16V	-2.20 ± 0.32	0.18 ± 0.26	0.11 ± 0.35	0.01 ± 0.11	0.04 ± 0.14	–	–	–
I18V	-1.17 ± 0.22	0.18 ± 0.12	-0.18 ± 0.27	-0.11 ± 0.11	0.18 ± 0.22	–	–	–
V30A	-4.88 ± 0.23	-0.61 ± 0.17	-1.95 ± 0.25	0.06 ± 0.04	0.36 ± 0.06	–	–	–
A40G	-1.71 ± 0.20	-0.30 ± 0.14	-0.12 ± 0.23	-0.03 ± 0.10	-0.11 ± 0.12	–	–	–
L50V	0.37 ± 0.23	0.18 ± 0.11	0.20 ± 0.29	-0.20 ± 0.74	-0.03 ± 0.87	–	–	–
I57V	-0.43 ± 0.22	0.34 ± 0.12	0.13 ± 0.27	-0.63 ± 0.39	-0.17 ± 0.51	–	–	–
V78A	-3.01 ± 0.17	-0.41 ± 0.10	-1.57 ± 0.20	0.03 ± 0.04	0.46 ± 0.08	–	–	–
L89V	-0.14 ± 0.23	0.06 ± 0.11	-0.31 ± 0.29	0.44 ± 0.44	1.49 ± 1.28	–	–	–
L95V	-0.75 ± 0.20	0.21 ± 0.14	0.16 ± 0.23	0.00 ± 0.15	0.07 ± 0.30	–	–	–
L16V/L95V	-2.01 ± 0.19	0.21 ± 0.11	-0.39 ± 0.23	–	–	-0.94 ± 0.42	0.18 ± 0.31	-0.12 ± 0.48
I18V/V78A	-5.06 ± 0.16	-1.33 ± 0.14	-2.28 ± 0.19	–	–	0.88 ± 0.32	1.10 ± 0.21	0.53 ± 0.39
A40G/L50V	-0.72 ± 0.23	-0.10 ± 0.16	0.08 ± 0.27	–	–	-0.62 ± 0.38	-0.02 ± 0.27	0.00 ± 0.46
V78A/L89V	-4.06 ± 0.32	-0.85 ± 0.26	-1.93 ± 0.34	–	–	0.91 ± 0.43	0.50 ± 0.30	0.05 ± 0.49

[a] Difference free energy changes between wild type (WT) and mutant (MUT) proteins calculated with the equation $\Delta\Delta G = \Delta G_{WT} - \Delta G_{MUT}$. [b] Difference free energy change between the transition state and unfolded state, $\Delta\Delta G_{t-U} = \Delta\Delta G_{F-U} - \Delta\Delta G_{F-t}$ [where $\Delta\Delta G_{F-t} = -RT \ln[k_{F-I(MUT)}/k_{F-I(WT)}]$]. [c] Φ values calculated using eq 5. [d] $\Delta G_{int(F)}$, $\Delta G_{int(I)}$, and $\Delta G_{int(t)}$ are the interaction free energies calculated for the folded, intermediate, and transition states, respectively. They were calculated according to the relationship (*30*) $\Delta G_{int} = \Delta\Delta G_A + \Delta\Delta G_B - \Delta\Delta G_{AB}$, where A and B denote the two single mutants and AB denotes the double mutant. Quoted errors are standard errors and were calculated from the data in Table 1 using the standard statistical formula.

average destabilizing effect on the folded state is 1.1 ± 0.7 kcal mol^{-1} per methylene group, a value consistent with those determined in other studies (*24*, and references therein).

Rate profiles (k_{obs} vs denaturant activity) collected for the mutants are plotted in Figure 2. As with wild type CD2.d1, all mutants fold through a transiently populated intermediate, as demonstrated by the change in slope of the folding limb from weak to strong folding conditions; i.e., the ground state associated with the major transition state changes from U (slope $= m_U - m_t$) to I (slope $= m_I - m_t$). The data have been fitted to eq 3, and the calculated values of $k_{I-F(W)}$, $k_{F-I(W)}$, $K_{I/U(W)}$, m_U, m_I, and m_t are given in Table 1. The calculated difference free energies for the intermediate ($\Delta\Delta G_{I-U}$) and the I-to-F transition state ($\Delta\Delta G_{t-U}$) are given in Table 2.

Stability of the I-State Secondary Structure Propensity. In stark contrast to the effects on the folded state, six out of nine single mutations are found to stabilize the intermediate with respect to the unfolded state (see Table 2). At face value, these stabilizing effects are difficult to rationalize, as each substitution involves a reduction in the amount of nonpolar surface area capable of being buried in a hydrophobically collapsed structure. However, inspection of the plot in Figure 3a reveals a marked relationship between the effect of the mutation on the stability of the I-state and the propensity of the substituted residue to adopt the appropriate region of Ramachandran ($\phi-\psi$ angle) space. In this plot, $\Delta\Delta G_{I-U}$ values for the single mutants have been plotted alongside the calculated free energy change due to changes due to alterations in β-propensity ($\Delta\Delta G_\beta$; see Analytical Procedures and eq 7 in the Discussion). A linear fit to the data according to the relationship $\Delta\Delta G_{I-U} = m\Delta\Delta G_\beta + c$ (plot not shown) gives a correlation factor (r) of 0.87, a slope close to unity ($m = 1.2 \pm 0.2$) and passes through the origin ($c = -0.02 \pm 0.06$ kcal mol^{-1}). Figure 3b shows the results for the I-to-F transition. The data, when fitted to the above relationship, are poorly correlated ($r = 0.50$) and yield values for the slope and intercept of 3.6 ± 1.6 and 1.5 ± 0.4 kcal mol^{-1}, respectively (not shown). These results suggest that backbone $\phi-\psi$ angle preferences play an important role in determining the structural and energetic properties of the rapidly formed intermediate but have little effect on the I-to-F transition. The direct correlation found between $\Delta\Delta G_{I-U}$ and $\Delta\Delta G_\beta$ also suggests that the interactions made by the deleted side chain groups with the rest of the protein must be relatively weak in the intermediate.

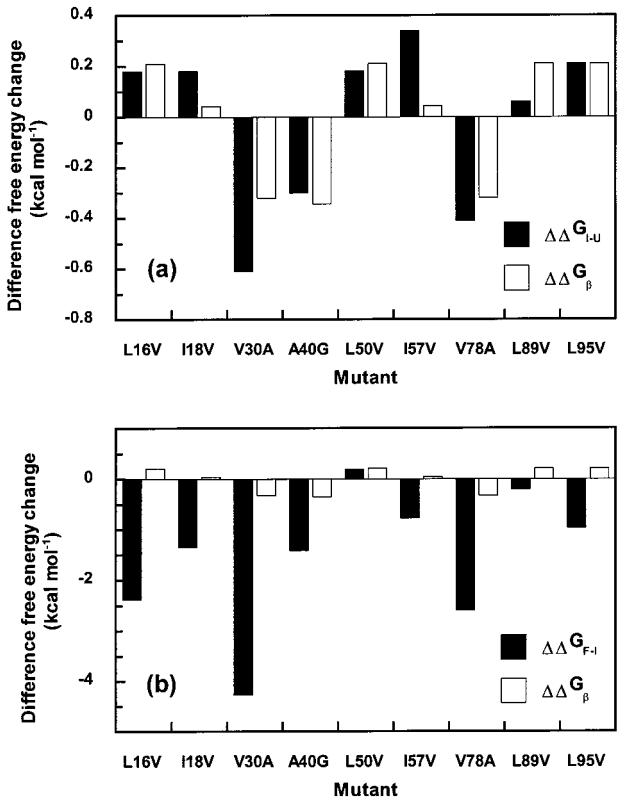

FIGURE 3: Correlation between changes in stability and changes in β-structure propensity. In panel a, the difference free energy changes measured for the U-to-I transitions of the single mutant CD2.d1 proteins ($\Delta\Delta G_{I-U}$; see Table 2) have been plotted against the expected difference free energy change due to changes in β-structure propensity ($\Delta\Delta G_\beta$, calculated using eqs 4 and 7). A similar plot is shown in panel b for the I-to-F transition (difference free energy change for the I-to-F transition, $\Delta\Delta G_{F-I} = \Delta\Delta G_{F-U} - \Delta\Delta G_{I-U}$; see Table 2).

Φ *Value Analysis.* A Φ value for a folding reaction describes the difference free energy measured for a given

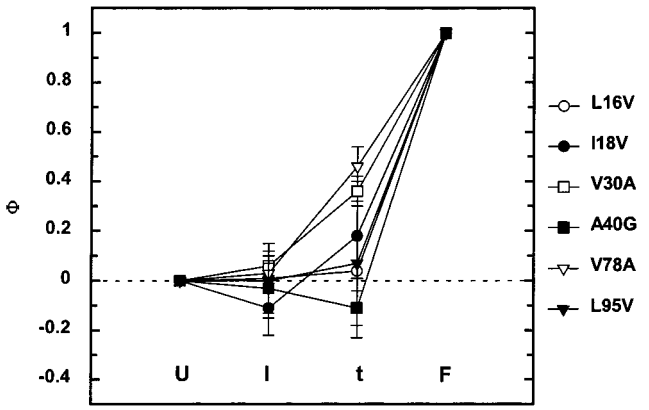

FIGURE 4: Φ value analysis. The Φ values for the intermediate and transition states (Φ_I and Φ_t, respectively), calculated using eq 5 and the results in Table 1, are illustrated graphically in this plot. Error bars are shown for the data (see Table 2). The Φ values calculated for L50V, I57V, and L95V have been omitted from this plot; the relatively large degrees of uncertainty in these values preclude their treatment.

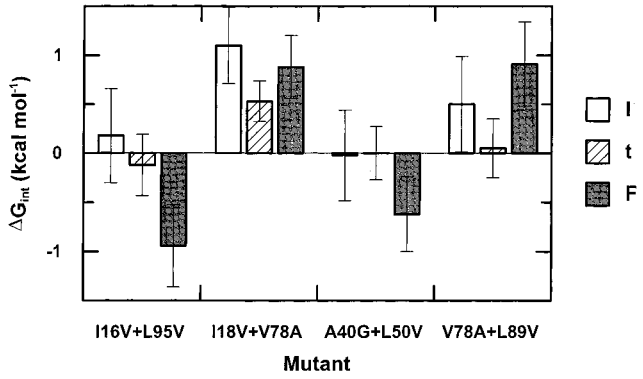

FIGURE 5: Double-mutant cycle analysis. The interaction free energies or coupling constants (ΔG_{int}) for the intermediate, transition, and folded states, calculated from the double-mutant cycles constructed for I16V/L95V, I18V/V78A, A40G/L50V, and V78A/L89V, are shown here in graphical form (see Table 2). Error bars are shown for the data.

state as a fraction of that measured for the fully folded state, i.e., the Φ value for state X ($\Phi_X = \Delta\Delta G_{X-U}/\Delta\Delta G_{F-U}$). For small, conservative side chain deletions of buried residues, Φ is taken to represent the fractional development of interactions made by the deleted moiety with the rest of the protein in the folded state (*30*). In this analysis, the unfolded molecule is taken as a reference state. This is justified by the argument that there are no organized noncovalent interactions in this state so that conservative side chain deletions of nonpolar residues will have a negligible effect on the free energy of this state compared with effects on the more conformationally ordered intermediate, transition, and folded states. However, the correlation found between $\Delta\Delta G_{I-U}$ and $\Delta\Delta G_\beta$ in Figure 3a prompts some modification of this basic assumption. That is, as the $\phi-\psi$ angle distribution within the unfolded state ensemble is affected by the substitutions, the free energy of this state can no longer be accepted as an exact reference.

Given that the ϕ and ψ angles of these residues are necessarily limited to our definition of the β-region (see Analytical Procedures and Table 1) in the I-, t-, and F-states and that $\Delta\Delta G_\beta$ describes, as a free energy, the change in preference for a given site within the unfolded ensemble to adopt this region of $\phi-\psi$ angle space then, the appropriate expression for Φ, as a measurement of the development of side chain contacts, should be as follows:

$$\Phi = (\Delta\Delta G_{X-U} - \Delta\Delta G_\beta)/(\Delta\Delta G_{F-U} - \Delta\Delta G_\beta) \quad (5)$$

The Φ values for the intermediate and transition states (Φ_I and Φ_t, respectively) calculated using this equation are given in Table 2. Unfortunately, for mutants L50V, I57V, and L95V, small values of $\Delta\Delta G_{F-U}$ lead to large errors in both Φ_I and Φ_t, thus precluding their use in the analysis. The Φ values for the remaining mutants, which have tolerable errors, are presented in graphical form in Figure 4. On the basis of the definition presented in eq 5, Φ_I values for these mutants are close to zero. In contrast, Φ_t values fall, broadly, into two classes: zero Φ_t values and intermediate Φ_t values ($\Phi_t = 0.2-0.5$). The results show that contacts made by the deleted side chain groups of L16, A40, and L95 are only detected in the fully folded state (former category), while those of I18, V30, and V78 make a measurable contribution to the rate-limiting transition state (latter category).

Double-Mutant Cycle Analysis. The discussion above highlights the potential problems encountered in using Φ values to give a direct measurement of the development of side chain−side chain contacts in protein folding reactions. A more rigorous and less ambiguous means of estimating the formation of specific side chain contacts involves using double-mutant cycles (*31*). By subtracting the combined free energy changes for two single mutations (A and B) from the free energy change in the double mutant (AB), we can deduce the specific contribution of the contact between the mutated side chains to the stability of any state in the folding reaction. While suffering more from accumulated errors than Φ value measurements, analysis by double-mutant cycles simplifies the assessment of pairwise interactions, as additional side chain interaction free energies and backbone $\phi-\psi$ angle preferences are effectively canceled out.

Double-mutant cycles have been constructed for L16V/L95V, I18V/V78A, A40G/L50V, and V78A/L89V. The interaction free energies and coupling constants (ΔG_{int}) for each state in the folding reaction are given in Table 2. The ΔG_{int} values are represented graphically in Figure 5. As can be seen, the results for A40G/L50V demonstrate the existence of a stabilizing contact between the side chains of these two residues in the folded state which is only measurably formed after the rate-limiting transition barrier has been traversed. This result agrees well with the Φ value analysis of A40G (see Figure 4; errors preclude analysis of Φ values for L50V). The results for L16V/L95V also reveal a stabilizing contact made between the side chains of L16 and L95 in the folded state which is only measurably formed once the transition barrier has been traversed. Similarly, these results are consistent with the Φ_I and Φ_t values measured for L16V and L95V (see Figure 4). Somewhat surprisingly however, the double-mutant cycles constructed for I18V/V78A and V78A/L89V reveal positive interaction free energies in the intermediate, transition, and folded states.

A positive interaction free energy is likely to arise from local strain in the structure which is compensated for by favorable contacts elsewhere. For instance, V78 is in a tightly packed environment in the core of the wild type molecule, but has an unfavorable, partially eclipsed χ_1 torsion angle

according to the crystal structure (*29*). The double-mutant cycle allows cancellation of all contact energies other than those between the participating side chains. However, if local strain is relieved in both single mutants and in the double mutant, then the contribution from this source will not cancel. In these circumstances, the interaction free energy (ΔG_{int}) will contain two terms: one negative (owing to hydrophobic contact energy) and one positive (owing to conformational strain). It is noticeable that the double-mutant cycles which show positive interaction energies both include the V78 residue, and further, all other members of the immunoglobulin V set (variable set) have a disulfide bond connecting positions 18 and 78 (*32*). The other residues which constitute the hydrophobic core of CD2.d1 are highly conserved in the immunoglobulin V set (*16*, *32*). It seems likely then that, within this general family of proteins, the core residues have evolved around this cystine structure and its replacement by a valine-isoleucine pair in CD2.d1 has incurred some degree of steric conflict despite the favorable net contribution of the individual residues to the stability of the folded state.

DISCUSSION

The results of this study suggest that side chain−side chain interactions are relatively weak in the rapidly formed I-state of CD2.d1 and that local secondary structure preferences play an important role in this early stage of structural acquisition. Estimates of the degree of solvation of the I-state, based on *m* values and heat capacity changes, suggest that ∼40−45% of the nonpolar groups buried in the core of the F-state are desolvated at this stage in the reaction (*17*). The relative weakness of side chain interactions in the I-state is presumably a consequence therefore of a significant number of intervening water molecules remaining in the hydrophobic core. However, the fact that steric clashes between residues I18 and V78, and V78 and L89, in the folded state are also apparent in the I-state (see Results) does suggest that the relative positions of these side chains are native-like at this stage of the reaction.

Secondary structural preferences appear to play a much reduced role in the rate-limiting I-to-F transition, which involves the intimate locking of side chains coupled with the final exclusion of water molecules from the core of the protein (*17*). The Φ_t values (see Figure 4) are shown in the context of the folded structure in Figure 6. It is interesting to note that the residues with non-zero Φ_t values (V30, I18, and V78; see Figure 4) are located in close spatial proximity on one side of the central core tryptophan residue, suggesting that the rate-limiting transition state is attained by the formation of a tightly localized hydrophobic nucleus which includes residues V30, I18, and V78. Interestingly, in all other members of the immunoglobulin V set, this part of the hydrophobic core contains a disulfide bridge (*32*); a structural feature which would serve as an effective stabilizer of this folding nucleus.

It should be noted that the above Φ value analysis is valid only when certain criteria are satisfied (*29*). First, mutations should not significantly alter the structure of the F- or U-states. Without high-resolution X-ray data, it is not possible to be certain about the structural effects of mutations on the folded molecule, but small aliphatic deletion mutations, like those used here, have previously been shown to lead to small cavities in the folded structure with no significant transmission of the perturbation to other regions of the structure (*33*). Furthermore, no mutant caused more than a 10% change in the value for m_u (Table 2), an observation which shows that the mutations do not have a large effect on the relative degree of solvated hydrocarbon between the U- and F-states. Second, mutant residues should not make any new interactions during any part of the folding process. None of the mutants presented here has new functional groups; therefore, it is unlikely that new interactions will have been introduced. Third, the mutations do not alter the folding pathway. For the mutants to be directed down an alternative folding pathway, the free energy of the activation barrier between I and F must be significantly altered. Since the mutant that has the greatest affect on the t-state only results in a 2 kcal/mol change in free energy of the activation barrier, it appears to be improbable that an alternative folding pathway would be available to the mutant proteins.

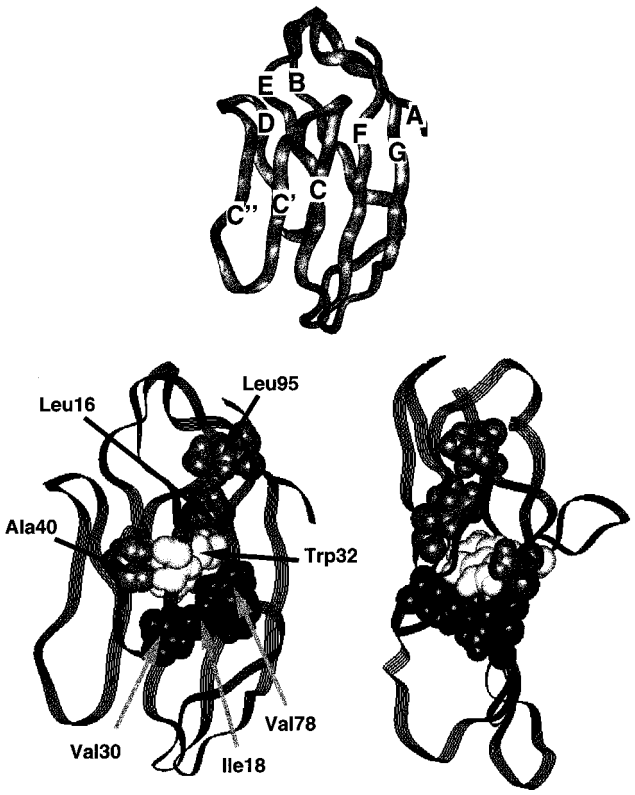

FIGURE 6: Folding nucleus in the transition state. The top picture shows the backbone topology of the CD2.d1 molecule (backbone represented by a solid ribbon) with the strand positions labeled. The Φ_t values measured for the single mutants (see Table 2 and Figure 5) are shown in the context of the CD2.d1 structure in the lower pictures (left-hand side, molecule in the same projection as in the top picture; right-hand side, 90° rotation of this image). The side chain atoms of the residues are represented by spheres. Residues with zero Φ_t values are dark gray, while those with fractional Φ_t values are black. The core tryptophan residue is also indicated (light gray).

With regard to the influence of the β-propensity on the formation of the I-state, the following arguments can be applied. The propensity of an amino acid to adopt a given region of Ramachandran space (region *x* say) can be determined statistically from a database of protein structures (*34*) and is derived from the following linked equilibria:

Scheme 2

$$U_{other} \overset{K_{ssp}}{\rightleftharpoons} U_x \overset{K_F}{\rightleftharpoons} F_x$$

Here K_{ssp} is an equilibrium ratio ($[U_x]/[U_{other}]$) describing the propensity of a particular amino acid in a random coil to adopt region *x* over all other regions of Ramachandran space. Region *x* is compatible with and fixed in the folded structure (F_x). Hence, K_F describes the additional stability afforded to this residue configuration in the context of the folded state. Evolution will select those residues which have the highest value of K_{ssp} appropriate to the folded structure but must also optimize for other (relatively more important) energetic criteria, such as packing constraints and hydrophobicity, to maximize the value of K_F. However, using a sufficiently large database, representing a wide variety of protein folds, the context dependence implicit in K_F is lost and the statistical occurrence in different conformations will then reflect K_{ssp} (see eq 4). This basic assertion has found support from a number of experimental studies, performed on peptide and protein systems, which have provided α-helix and *β*-sheet structure propensity scales which are in good agreement with statistical scales (*35*−*44*).

In terms of providing a rationale for these intrinsic preferences, it has been suggested, from hydrogen−deuterium exchange studies, that the *β*-sheet-forming tendencies stem from constraints imposed by steric conflicts between the side chain and the main chain (*45*). Similarly, for central α-helix positions, it has been postulated that steric clashes between the side chain and upstream hydrogen bonding peptide groups limit the conformations available to the side chain, leading to an entropic factor which determines the α-propensity (*46*).

From Scheme 2, the contribution made by secondary structure propensity to the measured folding equilibrium constant [$K_{F(m)}$] can be notationally separated:

$$K_{F(m)} = [F]/([I_{other}] + [I_x]) = K_F K_{ssp}/(1 + K_{ssp}) \quad (6)$$

The predicted free energy change upon mutation, due solely to changes in secondary structure propensity ($\Delta\Delta G_{ssp}$), can therefore be written as

$$\Delta\Delta G_{ssp} = -RT \ln\left[\frac{K_{ssp}(1 + K_{ssp}')}{K_{ssp}'(1 + K_{ssp})}\right] \quad (7)$$

where K_{ssp} and K_{ssp}' describe the propensities of the wild type and mutant residues, respectively, to adopt that region of Ramachandran space appropriate to the folded structure. However, while it is known that ϕ and ψ angles are fixed in the F-state, no such knowledge is available for the I-state. If ϕ and ψ angles are not fixed in this state, then Scheme 2 becomes random order, as shown in Scheme 3:

From this scheme, the measured U-to-I equilibrium ratio [$K_{I/U(m)}$] is given by $K_{I/U(m)} = ([I_x] + [I_{other}])/([U_x] + [U_{other}]) = K_{I/U}$. Hence, a change in K_{ssp} will not influence the U-to-I equilibrium. The direct correlation found between $\Delta\Delta G_{I-U}$ and $\Delta\Delta G_\beta$ (see Figure 3a) rules out such a possibility for the rapid U-to-I transition of CD2.d1, leading to the conclusion that the ϕ and ψ angles of the mutated residues are limited to the *β*-region in the I-state. As the mutated residue positions cover the *β*-strand regions of the CD2.d1 molecule fairly comprehensively, this result suggests that a significant proportion of *β*-structure is formed in this part of the reaction. In other words, the summed interactions which dictate the structure of the I-state are capable of overcoming the effects of mutations which introduce residues with a low *β*-propensity; i.e., they are "pulled" into the correct conformation when the I-state is formed.

$$\begin{array}{ccc} & K_{I/U} & \\ U_{other} & \rightleftharpoons & I_{other} \\ K_{ssp} \uparrow\downarrow & & \uparrow\downarrow K_{ssp} \\ U_x & \rightleftharpoons & I_x \\ & K_{I/U} & \end{array}$$

Much controversy exists concerning the properties of rapidly formed I-states and the contribution they make to the folding reaction. One suggestion, based on data from cytochrome *c*, is that these states are formed by the random and nonspecific association of nonpolar groups and that they simply represent the unfolded ensemble populated at low denaturant concentrations (*47*). In response to this assertion, we would cite the following experimental evidence that the I-state formed by CD2.d1 has a higher degree of native-like structure than would be expected from such a generalized chain contraction. First, the pattern of exchange protection in the I-state is consistent with the formation of native hydrogen bonding between both sequence-local and sequence-distant *β*-strands (*15*, *16*). Second, while the exclusion of solvent from the nonpolar surface should lead to a highly favorable entropic term for the formation of the I-state at physiological temperature, measurement shows that the entropy change associated with the U-to-I transition is close to zero (*17*). A compelling interpretation of this result is that the favorable entropy of desolvation is balanced by an unfavorable conformational entropy resulting from the increase in the extent of organization of the polypeptide chain. Last, the results presented in this study reveal that where tested the ϕ and ψ angles in the I-state of CD2.d1 are native-like. These factors, together with the experimental observation that ϕ and ψ angle distributions are unaffected by changes in denaturant concentration (*48*), make it unlikely that the U-to-I transition in CD2.d1 simply reflects the contration of a randomly configured chain in response to strong folding conditions.

REFERENCES

1. Kauzmann, W. (1959) *Adv. Protein Chem. 14*, 1−63.
2. Lim, W. A., and Sauer, R. T. (1989) *Nature 339*, 31−36.
3. Baldwin, R. L. (1989) *Trends Biochem. Sci. 14*, 291−294.
4. Karplus, M., and Weaver, D. L. (1994) *Protein Sci. 3*, 650−668.
5. Lesk, A. M., and Rose, G. D. (1981) *Proc. Natl. Acad. Sci. U.S.A. 78*, 4304−4308.
6. Dill, K. A. (1990) *Biochemistry 29*, 7133−7155.
7. Chan, H. S., and Dill, K. A. (1990) *Proc. Natl. Acad. Sci. U.S.A. 87*, 6388−6392.
8. Dill, K. A. (1985) *Biochemistry 24*, 1501−1509.

9. Roder, H., and Colón, W. (1997) *Curr. Opin. Struct. Biol. 7*, 15−28.
10. Clarke, A. R., and Waltho, J. P. (1997) *Curr. Opin. Biotechnol. 8*, 400−410.
11. Kiefhaber, T. (1995) *Proc. Natl. Acad. Sci. U.S.A. 92*, 9029−9033.
12. Mirny, L. A., Abkevich, V., and Shakhnovich, E. I. (1996) *Folding Des. 1*, 103−116.
13. Driscoll, P. C., Cyster, J. G., Campbell, I. D., and Williams, A. F. (1991) *Nature 353*, 762−765.
14. Parker, M. J., and Clarke, A. R. (1997) *Biochemistry 36*, 5786−5794.
15. Parker, M. J., Dempsey, C. E., Lorch, M., and Clarke, A. R. (1997) *Biochemistry 36*, 13396−13405.
16. Parker, M. J., Dempsey, C. E., Hosszu, L. L. P., Waltho, J. P., and Clarke, A. R. (1998) *Nat. Struct. Biol. 5*, 194−198.
17. Parker, M. J., Lorch, M., and Clarke, A. R. (1998) *Biochemistry 37*, 2538−2545.
18. Horton, R. M., and Pease, L. R. (1991) in *Directed Mutagenesis: A Practical Approach* (McPherson, M. J., Ed.) Chapter 11, Oxford University Press, Oxford, U.K.
19. Parker, M. J., Spencer, J., and Clarke, A. R. (1995) *J. Mol. Biol. 253*, 771−786.
20. Rost, B., and Sander, C. (1993) *Protein Eng. 6*, 831−836.
21. Shortle, D., Meeker, A. K., and Freire, E. (1988) *Biochemistry 27*, 4761−4768.
22. Staniforth, R. A., Burston, S. G., Smith, C. J., Jackson, G. S., Badcoe, I. G., Atkinson, T., Holbrook, J. J., and Clarke, A. R. (1993) *Biochemistry 32*, 3842−3851.
23. Myers, J. K., Pace, C. N., and Scholtz, J. M. (1995) *Protein Sci. 4*, 2138−2148.
24. Parker, M. J., Sessions, R. B., Badcoe, I. G., and Clarke, A. R. (1996) *Folding Des. 1*, 145−156.
25. Tanford, C. (1970) *Adv. Protein Chem. 24*, 1−95.
26. Pace, C. N. (1975) *CRC Crit. Rev. Biochem. 3*, 1−43.
27. Johnson, C. M., and Fersht, A. R. (1995) *Biochemistry 34*, 6975−6804.
28. Khorasanizadeh, S., Peters, I. D., and Roder, H. (1996) *Nat. Struct. Biol. 3*, 193−205.
29. Jones, E. Y., Davis, S. J., Williams, A. F., Harlos, K., and Stuart, D. I. (1992) *Nature 360*, 232−239.
30. Fersht, A. R., Serrano, L., and Matouschek, A. (1992) *J. Mol. Biol. 224*, 771−782.
31. Horovitz, A., and Fersht, A. R. (1990) *J. Mol. Biol. 214*, 613−617.
32. Barclay, A. N., et al. (1993) Protein superfamilies and cell surface molecules, in *The leucocyte antigen*, Academic Press, San Diego, CA.
33. Eriksson, A. E., Baase, W. A., Zhang, X. J., Heinz, D. W., Blaber, M., Baldwin, E. P., and Matthews, B. W. (1992) *Science 255*, 178−183.
34. Chou, P. Y., and Fasman, G. D. (1978) *Annu. Rev. Biochem. 47*, 251−276.
35. Kim, C. A., and Berg, J. M. (1993) *Nature 362*, 267−270.
36. Minor, D. L., and Kim, P. S. (1994) *Nature 367*, 660−663.
37. Smith, C. K., Withka, J. M., and Regan, L. (1994) *Biochemistry 33*, 5510−5517.
38. Lyu, P. C., Liff, M. I., Marky, L. A., and Kallenbach, N. R. (1990) *Science 250*, 669−673.
39. O'Neil, K. T., and DeGrado, W. F. (1990) *Science 250*, 646−651.
40. Padmanabhan, S., Marqusee, S., Ridgeway, T., Laue, T. M., and Baldwin, R. L. (1990) *Nature 344*, 268−270.
41. Merutka, G., Lipton, W., Shalongo, W., Park, S. H., and Stellwagen, E. (1990) *Biochemistry 29*, 7511−7515.
42. Creamer, T. P., and Rose, G. D. (1994) *Proteins: Struct., Funct., Genet. 19*, 85−97.
43. Horovitz, A., Matthews, J. M., and Fersht, A. R. (1992) *J. Mol. Biol. 227*, 560−568.
44. Blaber, M., Zhang, X. J., and Matthews, B. W. (1993) *Science 260*, 1637−1640.
45. Bai, Y., and Englander, S. W. (1994) *Proteins: Struct., Funct., Genet. 18*, 262−266.
46. Aurora, R., Creamer, T. P., Srinivasan, R., and Rose, G. D. (1997) *J. Biol. Chem. 272*, 1413−1416.
47. Sosnick, T. R., Shtilerman, M. D., Mayne, L., and Englander, S. W. (1997) *Proc. Natl. Acad. Sci. U.S.A. 94*, 8545−8550.
48. Plaxco, K. W., Morton, C. J., Grimshaw, S. B., Jones, J. A., Pitkeathly, M., Campbell, I. D., and Dobson, C. M. (1997) *J. Biomol. NMR 10*, 221−230.

BI9817820